

A NEW METHODOLOGY FOR DETERMINING INTERFACIAL SHEAR STRENGTH IN SINGLE FIBER COMPOSITES

Gale A. Holmes, Donald L. Hunston, Walter G. McDonough, and Richard C. Peterson

National Institute of Standards & Technology
Polymers Division, Polymer Composites Group
Gaithersburg, Maryland 20899-8543

ABSTRACT

Two of the critical factors controlling the long-term performance and durability of composites in structural applications is the fiber-matrix interfacial shear strength (IFSS) and the durability of the fiber-matrix interface. The single fiber fragmentation test (SFFT) has been viewed by many as the best method for determining these parameters. Although the SFFT has been extensively researched, the micro-mechanics models used to obtain IFSS values are based on simplifying assumptions that are usually not realized under experimental conditions. Thus, results from this test often violate the known strength of the constituent materials. Therefore, a new test method is presented here that utilizes realistic assumptions.

KEY WORDS: Interfacial Shear Strength, Single Fiber Fragmentation Test, Model

1. INTRODUCTION

The specific energy absorption characteristic (crashworthiness) is a primary factor in assessing the suitability of a structural composite for use in automotive applications. In contrast to metals and polymers, the crashworthiness of a composite is dependent on the fiber orientation, the loading conditions, the matrix properties, and the fiber-matrix interface strength. Currently, the crashworthiness of a composite is evaluated by crushing composite tubes in a controlled methodology, as a means of comparing the performance of real engineering structures during

crash tests. From these tests, the crashworthiness of a composite has been found to be enhanced by inducing microfracture throughout the material, at stresses close to the compressive strength of the material, using a chamfer trigger on the loading axis.[1] Tests have shown that the specific energy absorption of composites tested in this manner often exceed the specific energy absorption of conventional metallic materials. Without this triggering mechanism, the specific energy absorption of a composite is reduced considerably. Thus, for composites to be successfully introduced into automotive and other structural applications subject to impact, many other factors must be addressed, in particular, the effect of off-axis loading on the energy absorption characteristic of a composite.

To optimize a composite's performance and better understand the limitations inherent in composite structures subjected to impact loading, the failure mechanisms and the performance of the distinct phases must be understood and optimized. Although, the fiber and bulk matrix properties are readily obtained from standard tests, the interaction between these phases and the microscopic failure mechanisms that often precede macroscopic failure is often controlled by the properties of the fiber-matrix interface. Research by Hull *et al.* on glass cloth/epoxy composite tubes has shown that fiber-matrix interface properties can change the specific energy absorption of a composite by approximately 25 %. [2]

In the industrial environment, the fiber-matrix interface strength of a composite is generally assessed by macroscopic tests (e.g., short beam shear and Iosipescu shear). Due to the heterogeneous nature of composites, the strength and failure characteristics of composites are controlled by (1) fiber type, (2) resin type and degree of cure, (3) fiber architecture, (4) fiber volume fraction, (5) fiber misalignment, (6) void content, (7) fiber-matrix interface properties, and (8) localized composite stresses. Although these factors influence a composite's performance, interfacial shear strength results from these types of tests are process specific.

To overcome this inability to independently assess the fiber-matrix interface strength in a controlled manner, researchers have attempted to use micro-mechanics to predict the performance of a composite from its constituent materials and assess the strength and durability of the fiber-matrix interface. Since the fiber-matrix interface is not formed until the manufacturing process, a fast, inexpensive, and accurate method of assessing the properties of the fiber-matrix interface has been sought to facilitate this process. The success of such an approach would eliminate expensive re-testing when processing conditions and manufacturing equipment are changed. Since composite damage can initiate at the microstructure level, the ability to predict the onset of composite failure rests in the domain of the composite microstructure and the peak stresses that exist in the region of interest. In many cases, the region of interest is the fiber-matrix interface. Therefore, a microstructure approach, if successful, may allow the engineering of the desired interfacial properties at the supply level, via modification of the fiber surface. To this end, many micro-mechanics tests have been developed with the most notable being the SFFT.

In the SFFT, a single fiber is aligned along the axis of a dog bone cavity and embedded in a resin having an extension-to-failure that is typically 3 to 5 times higher than the fiber. The matrix is strained until the resulting fiber fragments are too short for sufficient loads to be transmitted into them to cause additional failure. This point is termed saturation. The lengths of the fragments at this point reflect the interface strength of the fiber-matrix interface. Although the

SFFT loads the fiber in a manner consistent with full-scale composites and captures the effect of Poisson's ratio contraction on the IFSS, this test ignores fiber-fiber interactions, void content, and the effect that residual stresses have on interface behavior. At best, this test, as currently formulated, offers a pristine view of the fiber-matrix interface. In addition, the interpretation of data from this test has been impeded by the tendency of researchers to use simplistic micro-mechanics models to account for matrix materials behavior. As a result, data analysis from a SFFT often yields results that exceed the known strength of the matrix. In addition, the results are suspect since the matrix material properties used to extract IFSS values are inconsistent with experimental data.

To address these problems, a call was issued for the development of realistic models for the SFFT to allow an accurate determination of the IFSS and assessment of the strengths and weaknesses of the test procedure. The research presented here is the first attempt at the development of such a procedure.

2. PROCEDURE

To perform the test as outlined here, it is recommended that one use a microscope and tensile stage based on the Drzal prototype and modified by the National Institute of Standards & Technology (NIST) (see Figure 1).[3],[4] The apparatus should be equipped with a load cell (1112 N) to measure the change in load with increasing strain and a device that monitors and records the load. The dimensions of a typical test specimen are shown in Figure 2. Two reference marks should be placed on the gauge section of the specimen (approx. 10 mm apart) and a suitable reference point should be found on each mark. The location of each reference point in the unstressed state must be recorded.

From previous research, it has been shown that the DGEBA/m-PDA matrix and other commonly used polymer matrices exhibit nonlinear viscoelastic behavior during fiber fracture.[4] Since this behavior is inconsistent with existing micro-mechanics models, it is recommended that the nonlinear viscoelastic micro-mechanics model developed at NIST be used to assess the IFSS. The general equation for calculating the IFSS from the experimental data is given below:

$$t_{interface} = \frac{d_f \mathbf{b}\{\mathbf{e}, t\}}{4} \left(\frac{\sinh(\mathbf{b}\{\mathbf{e}, t\} l_c / 2)}{\cosh(\mathbf{b}\{\mathbf{e}, t\} l_c / 2) - 1} \right) \mathbf{s}_f \{l_c\} \quad [1]$$

where

$$\mathbf{b}\{\mathbf{e}, t\} = \frac{2}{d_f} \left[\frac{E_m \{\mathbf{e}, t\}}{(1 + \mathbf{n}_m)(E_f - E_m \{\mathbf{e}, t\}) \ln \left(\frac{2r_m}{d_f} \right)} \right]^{1/2}$$

E_m, E_f are the matrix and fiber moduli, respectively.
 ν_m is the matrix Poisson's ratio
 d_f is the fiber diameter
 r_m is the radius of matrix parameter
 l_c is the critical transfer length at saturation
 $\sigma_f\{l_c\}$ is the strength of the fiber at l_c

This equation indicates that the IFSS obtained from the SFFT is dependent on testing rate via the strain rate dependence of the viscoelastic matrix!

Initially, two tests must be performed using different testing protocols (10 min and 1 h) to assess the rate sensitivity of the fiber-matrix interface. The 10 min and 1 h designations represent the hold time between successive strain increments (see Figure 3). The intermediate test protocol shown in Figure 3 begins with a 10 min hold time between strain increments. The hold time then increases to the time required to record the location of the fiber breaks. In each protocol, the specimens should be deformed (14 to 16) μm during each step-strain, and the step-strain should be applied over a time frame of (1.0 to 1.2) s. At each strain increment, the change in the location of the reference points on the reference marks must be recorded. The total strain at each step-strain is determined from these measurements. Saturation is achieved when the fiber break count in the gauge section (see Figure 2) remains constant for 0.6 % strain ((3 to 5) step-strains). Following this deformation scheme, the effective strain rate of the 10 min test is approximately 0.00014 min^{-1} and the effective strain rate of the 1 h test is approximately $0.000025 \text{ min}^{-1}$. For the epoxy resin specimens currently tested, the fragment distribution changes when the effective testing rate is increased to $0.000050 \text{ min}^{-1}$ (intermediate test protocol) (see Figure 3). Rate sensitivity tests by Netravali on a variety of epoxy resin/graphite fiber systems revealed no dependence of the fragment distribution to testing rate.[5] However, the slowest testing rate used by these authors (0.0007 min^{-1}) is faster than the fast test protocol used here.

For the 1 h test, at each step-strain the location of each fiber break should be recorded by at least two marks to delineate each debond region's size. A standard uncertainty of 1.2 μm or better should be achieved for each mark. At the end of both tests (10 min and 1 h) the location and size of the debond regions associated with fiber breaks should be measured while the specimen is under stress. The specimen should then be returned to zero stress. Since the matrix is viscoelastic, the zero stress state does not imply that the specimen is in the zero strain state. Therefore, when the specimen is initially returned to the zero stress state, the stress will immediately begin to rise again and one should let it equilibrate before the stress is again returned to zero. This process should be continued until no appreciable rise in the stress is detected. This process usually takes less than 24 h. Two examples of the matrix recovery process are shown in Figure 4 for an epoxy matrix and a polyurethane matrix. After 24 h, the location and size of the debond regions should be recorded in the unstressed state and the location of the reference points used to determine the strain in the sample recorded. From these measurements, the average strain in each fiber fragment, the average debond region strain, and the residual strain in the specimen at saturation can be determined. For all E-glass specimens currently tested, the debond region comprises less than 5 % of the total fragment length. Therefore, we ignore the contribution of debonded sections of the broken fiber fragments to the

average fiber strain. Although we recommend recording all of the breaks in the gauge section of the specimen, to conform with Saint-Venant's principle, only those fiber breaks in the central portion of the gauge section (region approximately (15 to 17) mm long) should be used for data analysis (see Figure 2).

So far, results from these tests have shown that the fragment distribution, and hence the interface shear strength, of E-glass/polymer SFFT specimens is dependent on the testing protocol.[6] In the tested cases, the fragments are shorter when the specimens are tested by the slow test protocol. This change in the fragment distribution with rate is counter to the behavior one would predict based solely on viscoelastic effects. The anomalous behavior has been explained in terms of the existence of stress concentrations at the end of fiber fragments that promote microscopic failure of the fiber-matrix interface when the epoxy resin SFFT specimens are tested too fast.[7] At the time of this writing, detailed analyses have only been conducted on E-glass type fibers. However, research by Galiotis,[8] using the seminal work of Carrara and McGarry[9] as a basis, has shown that this type of failure also occurs with carbon fiber/epoxy composites.

From the rate sensitivity tests, a decision about the appropriate testing protocol must be made. It is recommended that if the fast and slow test protocol distributions are distinguishable at the 95 % confidence level (p-value < 0.05) using analysis of variance (ANOVA), then the slowest test protocol (1 h) should be used. Regardless of the selected testing protocol, the testing protocol should be indicated with the reported interface values. In addition, the variation of the fragment distribution when the 10 min and 1 h test protocols are used should be reported.

To obtain an interfacial shear strength value using the nonlinear viscoelastic equation, four values are needed: (1) the critical transfer length, (2) the modulus, (3) the radius of matrix parameter (r_m), and (4) the strength of the fiber at the critical length. An approach for obtaining all four values from the testing data will now be described.

The critical transfer length, l_c , is obtained from the average of the fragment length distribution, $\langle l \rangle$, by using the following equation:

$$l_c = K \langle l \rangle = \frac{4}{3} \langle l \rangle \quad [2]$$

The value of 4/3 for K in the above equation is based on assumptions that (1) the fiber strength has constant strength (i.e., negligible variability), and (2) the matrix is perfectly plastic. The variability in the fiber strength is rarely negligible and researchers have shown that the matrix does not in general exhibit perfectly plastic behavior during the SFFT. Determination of an appropriate methodology for obtaining K is an active research topic [10], and we currently recommend the use of 4/3 for K until a definitive method for determining this parameter is adopted.

Data from SFFT(s) clearly indicate that the modulus at saturation is much lower than the linear elastic modulus that is commonly used in Cox-type models (see Figure 5). This is due to strain

softening in the nonlinear viscoelastic region. In addition, it is known that the stiffness of a viscoelastic material depends on the testing rate. Hence, we recommend the use of the secant modulus at saturation in the NIST model to capture changes in matrix stiffness due to testing rate and strain softening of the matrix in the nonlinear viscoelastic region. To obtain this modulus, the stress 10 s after the application of each step-strain should be plotted versus the current strain (see Figure 5). The secant modulus at saturation is obtained by dividing the stress at saturation by the current strain.

As a matter of expediency, the average measured strain in the fragments at the end of the test can be used to estimate r_m . A detailed analysis on the variation of r_m during the testing procedure can be found elsewhere.[7] Currently, two approaches have been used to obtain the average fragment strain at the end of the test. In the first approach, the measured fragment lengths in the stressed and unstressed states are averaged. Using these values the average strain at the end of the test is obtained. Alternatively, the average strain in each fragment can be calculated. Then the average of these average strains can be used to estimate r_m . Since these two estimates usually agree to within a fraction of 5 %, we recommend the first approach. An estimate of r_m can be obtained by equating the average strain at the end of the test to the following expression:

$$\langle \mathbf{e}_f \{z, \mathbf{e}, t\} \rangle_{measured} = \frac{E^*}{N} \mathbf{e} \sum_{i=1}^N \left[1 - \frac{\cosh \langle \mathbf{b} \{ \mathbf{e}, t \} \rangle (l/2 - z_i)}{\cosh \langle \mathbf{b} \{ \mathbf{e}, t \} \rangle l/2} \right] \quad [3]$$

where

$$E^* = \frac{(E_f - \langle E_m \{ \mathbf{e}, t \} \rangle_{sec\ ant})}{E_f}$$

$$\langle \mathbf{b} \{ \mathbf{e}, t \} \rangle = \frac{2}{d} \left[\frac{\langle E_m \{ \mathbf{e}, t \} \rangle_{sec\ ant}}{(1 + \mathbf{n}_m)(E_f - \langle E_m \{ \mathbf{e}, t \} \rangle_{sec\ ant}) \ln \left(\frac{2r_m}{d_f} \right)} \right]^{1/2}$$

In the above expression, the secant modulus at the end of the test is used and Poisson's ratio for the matrix is assumed to be 0.35. In addition, the diameter of the fiber is measured and the modulus of the elastic fiber is known. Since the average measured fragment strain is obtained relative to the average unstressed fragment length at the end of the test, this value is used for l . This leaves only one unknown in the above expression, r_m . To estimate r_m , the strain along the fiber fragment is calculated at 1 μm intervals and averaged. The value of r_m is adjusted until both sides of equation 3 are equal. In Table 1, two values of r_m are given based on the expressions for β derived by Cox and Nayfeh. Nairn's research suggests that the Nayfeh expression is the most appropriate. ([11])

Several methods have been developed to estimate the ‘in situ’ $\sigma_f\{l_c\}$ using data obtained from the SFFT.[10] In all of the approaches, the constant shear stress (elastic-perfectly plastic) approximation is assumed and the Weibull distribution for fiber strength is assumed to follow the Weibull Poisson’s model for flaws along the fiber. Since the constant shear stress approximation is not a good approximation for most polymeric materials, a graphical approach is used here to estimate $\sigma_f\{l_c\}$. By using the following equation, the fiber stress profile in a hypothetical fiber fragment that has the diameter of the real fiber and a length much larger than the transfer length (approx. 20 mm) is calculated for each strain increment.

$$s_f\{z, \mathbf{e}, t\} = (E_f - \langle E_m\{\mathbf{e}, t\} \rangle_{sec\ ant}) \mathbf{e} \left[1 - \frac{\cosh\langle \mathbf{b}\{\mathbf{e}, t\} \rangle (l/2 - z)}{\cosh\langle \mathbf{b}\{\mathbf{e}, t\} \rangle l/2} \right] \quad [4]$$

At each strain increment, the current secant modulus is used along with the value of r_m determined above. In cases where stress concentrations significantly reduce the bonding efficiency at the fiber-matrix interface during the test, r_m should be considered an ‘effective’ r_m . The critical transfer length is taken to be the distance along the fiber where 96.55 % of the maximum fiber stress is reached. When the location of the fiber breaks at a given strain increment are compared with the transfer length, no fragmentation occurs in this stress-transfer region. The pseudo-exclusion zone behavior in the stress-transfer region suggests that these regions should be thought of as microscopic sample grips. Therefore, when a fiber-fragment of length 600 μm with a stress transfer region ($l_c/2$) equal to 150 μm breaks, what is actually being tested is the strength of a fragment 300 μm in length. Using this argument, the strength of a fiber of critical transfer length l_c can only be assessed in the SFFT by finding the strain at which fiber fragments of length $2(l\{\epsilon_i, t\}/2) + l_c$ breaks, where $l\{\epsilon_i, t\}$ is the critical transfer length at a given strain increment. To estimate the fiber strength from the existing test data, we assume that the decrease in the average fiber length with increasing strain represents the most probable failure strain for a fragment of that length. Therefore, the intersection point of the average fragment length versus strain plot with a plot of $2(l\{\epsilon_i, t\}/2) + l_c$ yields the failure strain of a fragment of critical transfer length l_c (see Figure 6). Multiplying the failure strain times the modulus of the E-glass fiber (67.5 GPa) yields the ‘in situ’ $\sigma_f\{l_c\}$. As a point of reference typical values obtained by this method are compared in Table 2 with the simplest numerical approach as prescribed by Phoenix *et al.* [10] Standard uncertainties for the values reported in Table 2 are not known at this time. These values, however, are also consistent with recent results by Thomason and Kalinka on E-glass fibers in the size range of (300 to 400) μm . [12]

Using these values the IFSS can now be determined. Typical values using this approach are shown in Table 3. Note that the values obtained from the NIST model are generally a fraction 19 % below the values obtained by the Cox model. In addition, the values from the NIST model are less than the ultimate tensile strength of the matrix. Although we used the estimates of fiber strength and r_m in the Cox model, these values cannot be obtained from the Cox model using the approaches described here. These results also agree with those obtained by Galiotis for moderately bonded epoxy/fiber interfaces.[8]

3. REFERENCES

1. D. Hull, Sci. & Tech. Rev. (1988).
2. H. Hamada, J.C. Coppola, and D. Hull, Composites , 23, 93 (1992).
3. L. T. Drzal and P. J. Herera-Franco, "Composite Fiber-Matrix Bond Tests," in Engineered Materials Handbook: Adhesives and Sealants, (ASM Int., Metals Park, Ohio , 1990), p. 391.
4. G. A. Holmes, R. C. Peterson, D. L. Hunston, W. G. McDonough, and C. L. Schutte, "The Effect of Nonlinear Viscoelasticity on Interfacial Shear Strength Measurements," in Time Dependent and Nonlinear Effects in Polymers and Composites, R. A. Schapery, Ed., (ASTM, 1999), p. 98.
5. A. N. Netravali, R. B. Hestenburg, S. L. Phoenix, and P. Schwartz, Polymer Composites, 10 , 226 (1989).
6. G. A. Holmes, R. C. Peterson, D. L. Hunston, and W. G. McDonough, Polymer Composites, (2000).
7. G. A. Holmes, Compos. Sci. Technol., (2000).
8. H. Jahankhani and C. Galiotis, J. Comp. Mater., 25, 609 (1991).
9. A. S. Carrara and F. J. McGarry, J. Comp. Mater. , 2, 222 (1968).
10. C.-Y. Hui, S. L. Phoenix, and D. Shia, Compos. Sci. Technol., 57, 1707 (97 A.D.).
11. J. A. Nairn, Mechanics of Materials, 26, 63 (1997).
12. J. L. Thomason and G. Kalinka, Gordon Research Conference on Composites, Ventura, CA. (2000)

Table 1

Theoretical Calculation of r_m

| Variables | Intermediate Test Protocol | Slow Test Protocol |
|--|-----------------------------------|---------------------------|
| Strain at End of Test | 4.04 % | 4.27 % |
| Avg. Fragment Length | 359 μm | 322 μm |
| Avg. Fiber Strain | 1.996 % | 1.963 % |
| Secant Modulus | 1.664 GPa | 1.382 GPa |
| Matrix Poisson's Ratio | 0.35 | 0.35 |
| Fiber Diameter | 16.07 | 14.74 |
| Est. Value of β_{Cox} & β_{Nayfeh} | 10.88 | 11.12 |
| r_m via β_{Cox} | 9.30 μm | 7.39 μm |
| r_m via β_{Nayfeh} | 26.32 μm | 17.84 μm |

Table 2

Sample Calculations of Fiber Strength at Saturation

| Specimen | Graphical Approach | Weibull Approach |
|-------------------------------------|--------------------|------------------|
| Intermediate Test Protocol Sample 1 | 1.836 GPa | 1.845 GPa |
| Intermediate Test Protocol Sample 2 | 1.411 GPa | 1.478 GPa |
| Intermediate Test Protocol Sample 3 | 1.580 GPa | 1.463 GPa |
| Intermediate Test Protocol Sample 4 | | 1.512 GPa |
| Slow Test Protocol Sample 1 | 1.517 GPa | 1.474 GPa |
| Slow Test Protocol Sample 2 | 1.553 GPa | 1.474 GPa |
| Slow Test Protocol Sample 3 | | 1.522 GPa |
| Slow Test Protocol Sample 4 | | 1.493 GPa |

Table 3

Theoretical Calculations of IFSS

| Variables & Outputs | Intermediate Test Protocol | Slow Test Protocol |
|--------------------------------------|----------------------------|--------------------|
| Critical Fiber Length, μm | 507 | 434 |
| Fiber Strength, GPa | 1.59 | 1.53 |
| Elastic Modulus, GPa | 3.06 | 3.06 |
| Cox Model, MPa | 79 | 95 |
| Secant Modulus, GPa | 1.71 | 1.69 |
| NIST Model, MPa | 64 | 77 |
| % Reduction | 19 % | 19 % |
| Kelly-Tyson, MPa | 22 | 26 |

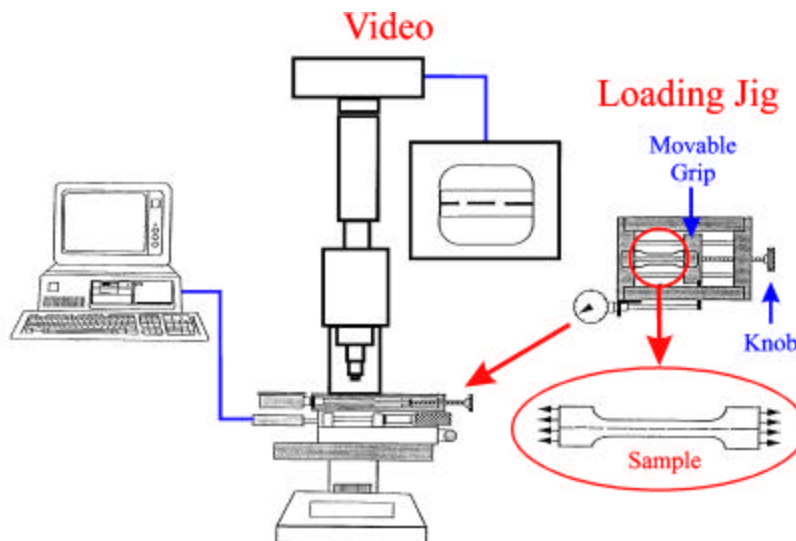


Figure 1. Schematic of Testing Apparatus.

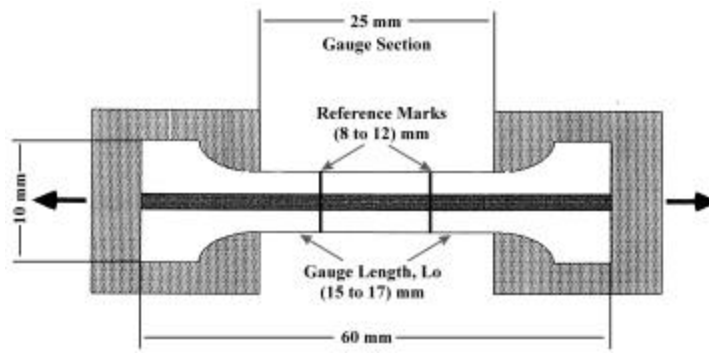


Figure 2. Typical Specimen Dimensions.

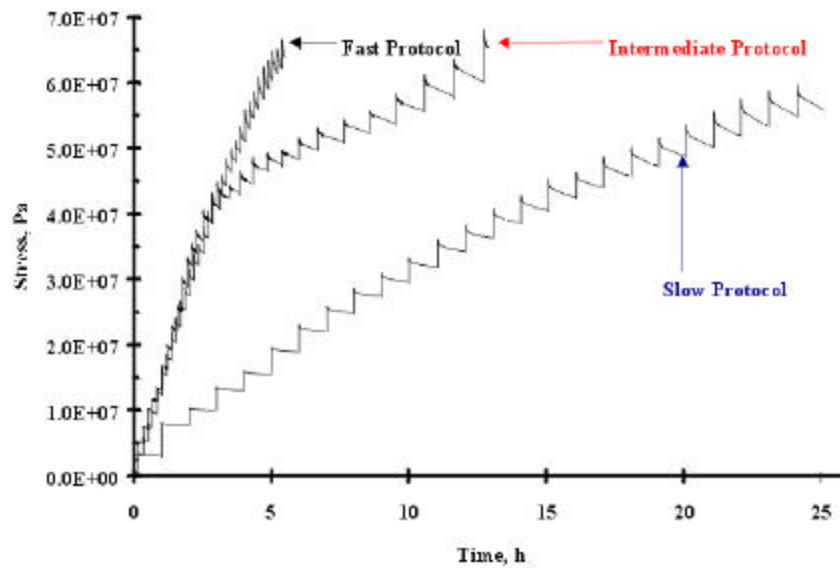


Figure 3. Stress-Time Curves for Test Protocols.

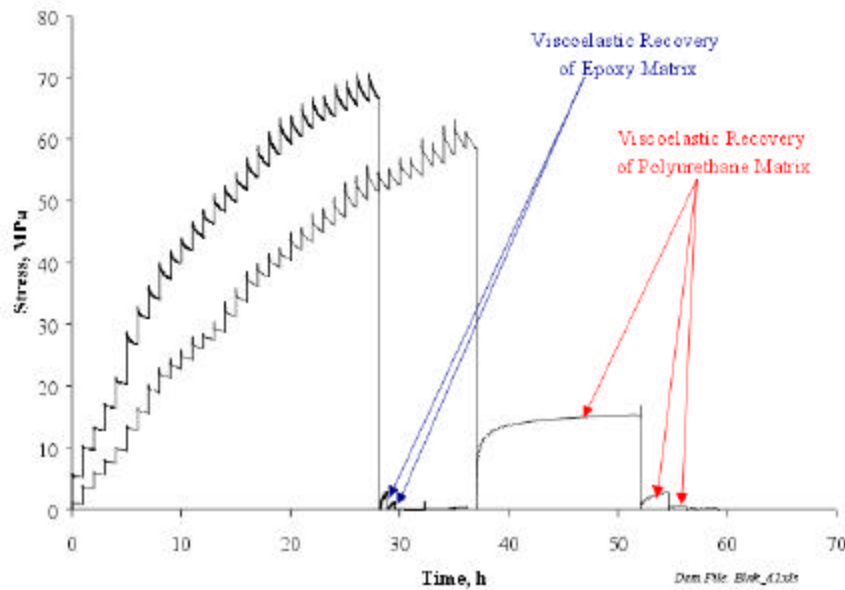


Figure 4. Matrix Recovery Profiles for Epoxy and Polyurethane Matrices.

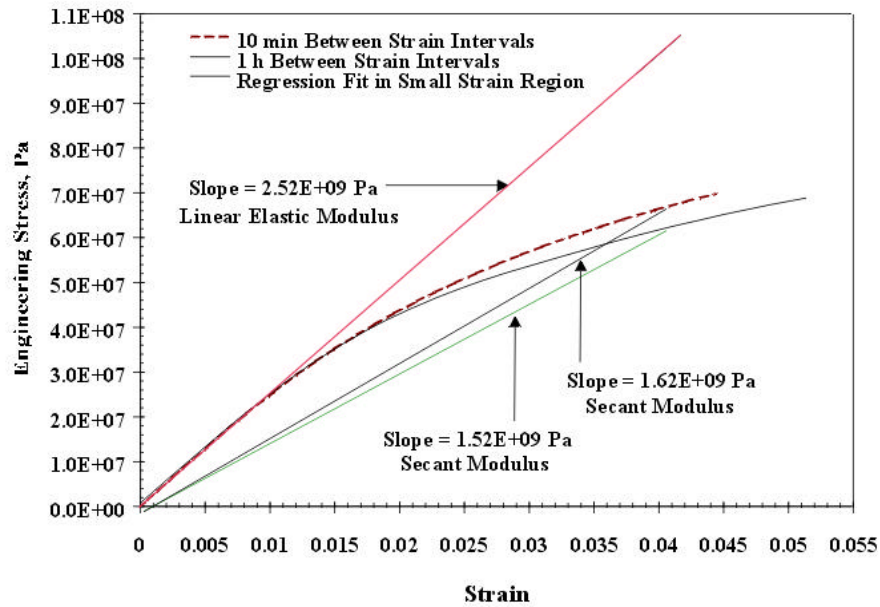


Figure 5. Typical Stress-Strain Plots from 10 min. and 1 h Test Protocol Specimens.

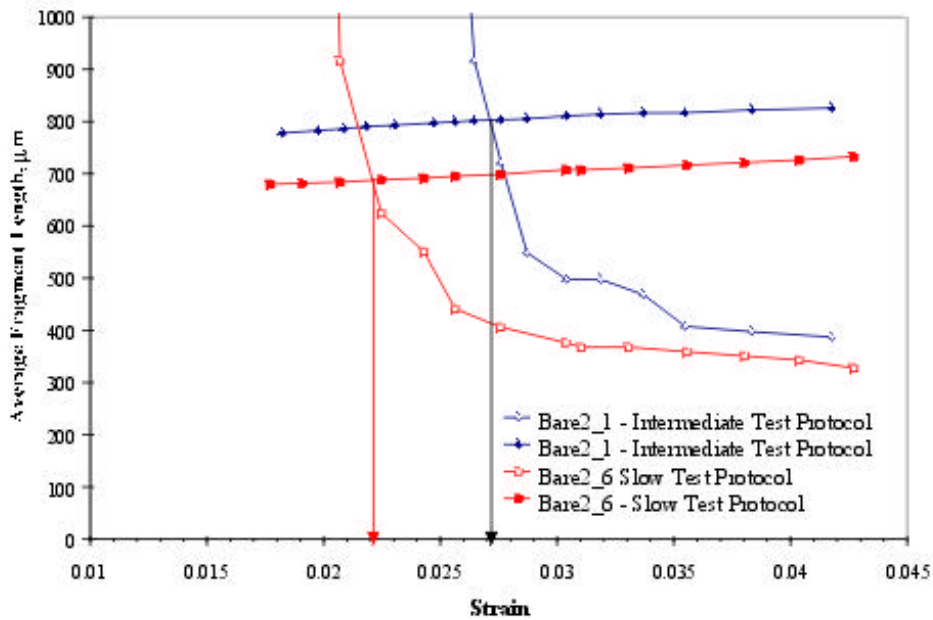


Figure 6. Graphical Determination of the 'in situ' Fiber Strength at Saturation from SFC Test Data.